PIGA (*N*,*N*-Di-*n*-butyl-5-chloro-2-(4-chlorophenyl)indol-3-ylglyoxylamide), a New Mitochondrial Benzodiazepine-Receptor Ligand, Induces Apoptosis in C6 glioma Cells

Beatrice Chelli,[a] Leonardo Rossi,[b] Eleonora Da Pozzo,[a] Barbara Costa,[a] Francesca Spinetti,[a] Mariarosa Rechichi,[b] Alessandra Salvetti,[b] Annalisa Lena,[b] Francesca Simorini,[c] Renato Vanacore,[d] Fabrizio Scatena,[d] Federico Da Settimo,[c] Vittorio Gremigni,[b] and Claudia Martini*[a]

Mitochondrial benzodiazepine-receptor (mBzR) ligands constitute a heterogeneous class of compounds that show a pleiotropic spectrum of effects within the cells, including the modulation of apoptosis. In this paper, a novel synthetic 2-phenylindol-3-ylglyoxylamide derivative, N,N-*di*-n-*butyl-5-chloro-2-(4-chlorophenyl)indol-3-ylglyoxylamide (PIGA), *which shows high affinity and selectivity for the mBzR, is demonstrated to induce apoptosis in rat C6 glioma cells. PIGA was able to dissipate mitochondrial transmembrane potential ($\Delta\Psi$m) and to cause a significant cytosolic accumulation of cytochrome c. Moreover, typical features of apoptotic cell death, such as caspase-3 activation and DNA fragmentation, were also detected in PIGA-treated cells. Our data expand the knowledge on mBzR ligand-mediated apoptosis and suggest PIGA as a novel proapoptotic compound with therapeutic potential against glial tumours, in which apoptosis resistance has been reported to be involved in carcinogenesis.*

Introduction

Apoptosis deregulation in gliomas, as in other tumours, is thought to be involved both in carcinogenesis and in the development of chemo- and radiotherapy resistance.[1] The opening of the mitochondrial permeability transition (MPT) pore, a multiprotein complex located at the contact site between the inner and outer mitochondrial membranes, has been suggested to be a key event in the apoptotic process.[2] mBzR has been suggested to be associated with this as an important component of this pore[3] and it has been extensively reported that classical mBzR ligands such as benzodiazepines (Ro5–4864)[4] and isoquinolines (PK 11195)[5] induce apoptosis, acting either as antitumour molecules themselves[6–11] or as chemosensitizing agents.[12–14]

Furthermore, novel mBzR ligands have been demonstrated to overcome apoptosis resistance; this suggests mBzR as a target for the development of new anticancer therapies.[15] The benzazepine BBL22 has been shown to induce apoptosis by arresting a variety of epithelial and haematological human tumours in the G2/M phase of the cell cycle.[16] Among indoleacetamides, the derivative FGIN-1–27 has been documented to decrease $\Delta\Psi$m, to activate caspase-3 and to cause DNA fragmentation.[8]

The design, synthesis and biological study of new mBzR ligands to obtain compounds with enhanced activity are an ongoing research project in our group. We have recently reported the synthesis and the binding affinities of a new class of potent and selective mBzR ligands: *N*,*N*-dialkyl-2-phenylindol-3-ylglyoxylamide derivatives,[17] which have been designed as conformationally constrained analogues of 2-phenylindole-3-ylacetamides such as FGIN-1–27.[18]

In this study we characterized (in rat glioma cells) the proapoptotic activity of the newly synthesized mBzR ligand *N*,*N*-di-*n*-butyl-5-chloro-2-(4-chlorophenyl)indol-3-ylglyoxylamide (PIGA),[17] chosen from the most potent ligands of the *N*,*N*-dialkyl-2-phenylindol-3-ylglyoxylamide series.[17]

Results and Discussion

Chemical Synthesis

The synthesis of PIGA was carried out essentially by following our previously reported procedure, with slight modifications (Scheme 1).[17] In brief, 5-chloro-2-(4-chlorophenyl)indole (**2**) was obtained through Houlihan modification of the Madelung

[a] *Dr. B. Chelli,[+] Dr. E. Da Pozzo, Dr. B. Costa, Dr. F. Spinetti, Prof. C. Martini*
Department of Psychiatry, Neurobiology, Pharmacology and Biotechnology
University of Pisa, Via Bonanno 6, 56126 Pisa (Italy)
Fax (+39) 050-221-9609
E-mail: cmartini@farm.unipi.it

[b] *Dr. L. Rossi,[+] Dr. M. Rechichi, Dr. A. Salvetti, Dr. A. Lena, Prof. V. Gremigni*
Department of Human Morphology and Applied Biology
University of Pisa, Via Volta 4, 56126 Pisa (Italy)

[c] *Dr. F. Simorini, Dr. F. Da Settimo*
Department of Pharmaceutical Sciences, University of Pisa
Via Bonanno 6, 56126 Pisa (Italy)

[d] *Dr. R. Vanacore, Dr. F. Scatena*
U.O. Immunohaematology 2, "Cisanello" Hospital
Via Paradisa 2, Pisa (Italy)

[+] *These authors contributed equally to this work.*

Supporting information for this article is available on the WWW under http://www.chembiochem.org or from the author.

  DOI: 10.1002/cbic.200400350

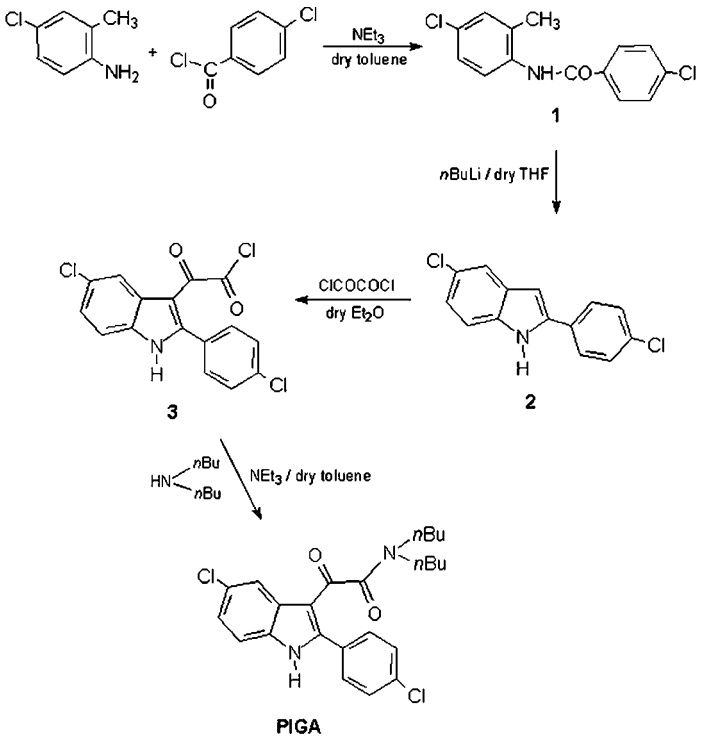

Scheme 1. The chemical synthesis of PIGA.

48 h (Figure 1). A PIGA concentration of 25 μM was therefore used for subsequent experiments.

The viability of untreated control cells after each incubation period was always greater than 90%, as determined by trypan blue exclusion assay (data not shown).

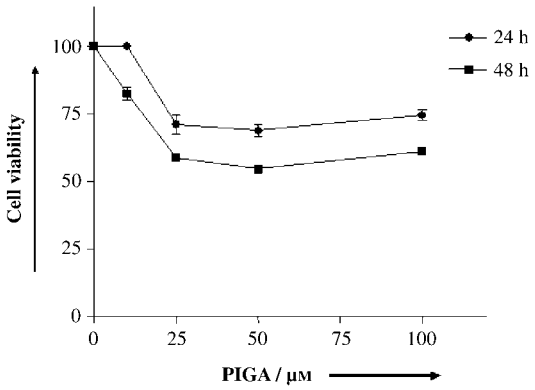

Figure 1. C6 glioma cell viability inhibition by PIGA: C6 glioma cells were treated with increasing concentrations (ranging from 10 to 100 μM) of PIGA for 24 h and 48 h. After incubation, cell viability was measured by MTS conversion assay as described in the Experimental Section. The results are expressed as a percentage of viable cells observed after treatment with PIGA vs untreated control cells (100%) and shown as mean ± SEM. The data are obtained from at least three separate experiments done in duplicate.

indole synthesis[19] from 4-chloro-*N*-(4-chloro-2-methylphenyl)-benzamide (**1**), in turn obtained simply by treating 4-chloro-2-methylaniline with 4-chlorobenzoyl chloride in dry toluene solution in the presence of triethylamine. Crude **2** was efficiently purified on Biotage Flash 40i (cyclohexane/ethyl acetate 85:15); this allowed us to obtain a pure sample in 85% yield. Intermediate **2** was acylated with oxalyl chloride in anhydrous ethyl ether at 0°C to give the corresponding indolylglyoxylyl chloride **3**, which upon treatment with di-*n*-butylamine in the presence of triethylamine in dry toluene solution afforded a crude sample of PIGA, which was purified by recrystallization from cyclohexane (yield 90%). *N*-*n*-Propyl-2-phenylindol-3-yl-glyoxylamide and 1-(2-phenyl-1*H*-indol-3-yl)-2-pyrrolidin-1-yl-ethane-1,2-dione were prepared essentially by following our previously reported procedure[17] (see Supporting Information).

Cell-viability inhibition

To test the ability of the mBzR-specific ligand PIGA to induce cell death, rat C6 glioma cells were treated with increasing concentrations of PIGA for 24 h and 48 h. Cell viability was then quantitatively measured by MTS conversion assay [MTS = 3-(4,5-dimethylthiazol-2-yl)-5-(3-carboxymethoxyphenyl)-2-(4-sulfophenyl)-2*H*-tetrazolium]. PIGA did not affect cell survival at nanomolar concentrations (data not shown), whereas micromolar ligand concentrations (from 10 to 100 μM) inhibited cell survival in a concentration-dependent manner. The maximum effect was recorded at a concentration of 25 μM: cell viability was reduced to 71.0 ± 3.5% at 24 h and to 58.8 ± 0.95% at

Among compounds structurally related to PIGA, the mBzR-selective and low-binding-affinity derivative 1-(2-phenyl-1*H*-indol-3-yl)-2-pyrrolidin-1-ylethane-1,2-dione (compound **10** in ref. [17]; $K_i = 2400 \pm 125$ nM for mBzR and $K_i > 10$ μM for BzR) and the low affinity and selectivity derivative *N*-*n*-propyl-2-phenylindol-3-ylglyoxylamide (see compound **1** in ref. [17]; $K_i = 815 \pm 80$ nM for mBzR and $K_i = 3929 \pm 381$ nM for BzR)[17] did not affect glioma cell viability even at the highest tested concentration (100 μM). Moreover, the unselective mBzR compound Diazepam and the central-type site-selective benzodiazepine Clonazepam did not induce significant reduction of glioma cell survival, as previously demonstrated by Chelli et al.[11] These findings support a correlation between the affinity of mBzR ligands and their antiproliferative activity. Nevertheless, PIGA induced an antiproliferative effect at concentrations significantly higher than those expected from its nanomolar affinity for the receptor. This quantitative discrepancy has previously also been reported for mBzR ligands in several cell lines.[11,16,20–23] It is known that ligand concentrations required to stimulate intracellular receptors may exceed those needed to saturate the same receptor by three orders of magnitude.[24] Other studies have suggested the possibility that mBzR ligands may inhibit cell survival in a mBzR-independent manner.[25–27] Our observations that the non-site-selective mBzR ligand Diazepam and the central-type benzodiazepine Clonazepam[11]—as well as the low mBzR affinity 2-phenylindol-3-ylglyoxyl-amides—did not affect glioma cell survival suggest a mBzR specificity of the PIGA effect.

Cell-cycle arrest

Flow cytometry was employed to determine whether PIGA caused a stage-specific inhibition of the cell cycle. After 24 h cell exposure, 25 μM PIGA had induced a significant accumulation of C6 glioma cells in the G0/G1 and G2/M phases, with a concomitant decrease in the proportion of cells in the S phase (Table 1), suggesting arrest of the cell cycle in the G0/G1 and G2/M phases. The cell cycle-modulating effects of mBzR ligands have been shown in previous studies.[8,16,26,28] As in our present study, concomitant arrest of the cell cycle in both G0/G1 and G2/M phases has also been demonstrated for the specific mBzR ligand PK 11195 in melanoma and breast cell lines.[20,21]

Table 1. The effect of PIGA on the cell cycle of C6 glioma cells.

	Percentage of cells in each phase of the cell cycle		
	G0/G1	S	G2/M
Control	61.6 ± 0.30	23.7 ± 0.24	14.7 ± 0.36
PIGA	64.4 ± 0.49[a]	18.2 ± 0.88[b]	17.4 ± 0.54[c]

C6 glioma cells were seeded at appropriate density into 24-well plates to ensure they had not reached confluency. After 24 h they were incubated either in the absence (control) or in the presence of 25 μM PIGA. After 24 h, the percentage of cells in each phase of the cell cycle was determined by flow cytometry as described in the Experimental Section. The values represent the means ± SEM. Data are obtained from at least three separate experiments done in duplicate. [a] $P < 0.01$ (vs. control, G0/G1 value). [b] $P < 0.001$ (vs. control, *S* value). [c] $P < 0.01$ (vs. control, G2/M value) one-way ANOVA (Newman–Keuls test).

mBzR subcellular localization

Since it is known that the receptor is differentially localized in different tumour cells,[29,30] we analysed mBzR subcellular distribution in C6 glioma cells. Immunolabelling data showed mBzR to be distributed throughout the cytoplasm, with preferential localization in the perinuclear region (Figure 2A, E). The mBzR subcellular distribution pattern, as evidenced by the specific fluorescent mBzR dye NBD-FGIN-1–27, correlated well with the distribution of the anti-mBzR antibody reactivity (Figure 2D). Subcellular localization of mitochondria, as evidenced by anti-cytochrome c antibody (Figure 2B), overlapped the pattern of mBzR staining (Figure 2C). Conversely, no nuclear mBzR labelling was observed with the specific nuclear envelope marker anti-lamin A antibody (Figure 2F, G). These data showed the receptor to be present at the mitochondrial level in rat C6 glioma cells, consistently with its most widely reported localization,[3] and pointed to mitochondrial membranes as the primary target for mBzR ligands in this cell line.

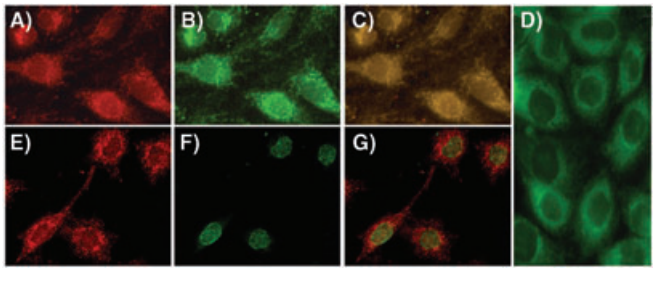

Figure 2. Assessment of the subcellular distribution of mBzR in C6 glioma cells by fluorescent microscopy. A) Distribution of mBzR as visualized by use of an anti-mBzR antibody. B) Subcellular distribution of mitochondria as revealed by use of an anti-cytochrome c antibody. C) Merged panels A and B demonstrate that mBzR is almost totally localized in the mitochondria. D) Subcellular distribution of mBzR as visualized by use of the specific ligand NBD-FGIN-1–27. E) Distribution of mBzR visualized by use of an anti-mBzR antibody. F) Nuclear envelope as visualized by use of an anti-lamin A antibody. G) Merged panels E and F demonstrate that mBzR is almost completely absent in the nuclear envelope.

Mitochondrial transmembrane potential dissipation and swelling

The effects of PIGA on $\Delta\Psi$m dissipation and mitochondrial swelling were investigated by flow cytometric analysis, with the use of the mitochondrial potentiometric probe JC-1 (5,5′,6,6′-tetrachloro-1,1′,3,3′-tetraethylbenzimidazolecarbocyanine iodide) and by ultrastructural observations, respectively. A decrease in $\Delta\Psi$m was evidenced by a reduction in orange JC-1 aggregate fluorescence (recorded by the FL 2 channel), accompanied by a concomitant increase in green JC-1 monomer fluorescence (recorded by the FL 1 channel).

Representative examples of cytometric analysis are given in Figure 3A. The vast majority of untreated control cells (96.1%) showed high fluorescence emission in both channels and were found in the upper right (UR) quadrant of the plot. The remaining 3.90% of untreated control cells showed low emission of fluorescence in FL 2, therefore plotting in the lower right (LR) quadrant. An increase in the percentage of cells plotting in the LR quadrant (17.8%), consistent with $\Delta\Psi$m dissipation, was seen in cells exposed to 25 μM PIGA for 24 h. In particular, significant changes in $\Delta\Psi$m were observed after treatment for graded time periods (3–48 h) starting from 24 h, as shown in Figure 3B. As a positive control, we used the uncoupling agent CCCP (carbonylcyanide *m*-chlorophenylhydrazone; 5 μM), and 69.2% of cells were found in the LR quadrant of the plot (Figure 3A).

Moreover, transmission electron microscopy (TEM) analysis revealed that the exposure to PIGA had caused mitochondrial damage. Untreated control cells showed mitochondria with electrondense matrices and well detectable cristae (Figure 4A), whereas cells incubated with 25 μM PIGA for 24 h or 48 h exhibited swollen and pale mitochondria with distorted cristae (Figure 4B).

Cytochrome c release

Glioma cell exposure to 25 μM PIGA for 24 h caused a significant release of cytochrome c, as revealed by comparing the specific immunoreactive bands in the mitochondrial and cytosolic fractions. The amount of cytochrome c in cytosol fractions of treated cells was 33.0 ± 7.90% ($P < 0.01$), as compared to 2.11 ± 1.12% in untreated control. In addition, cytochrome c was also detected in the cytosol from cells exposed to 3.8 mM

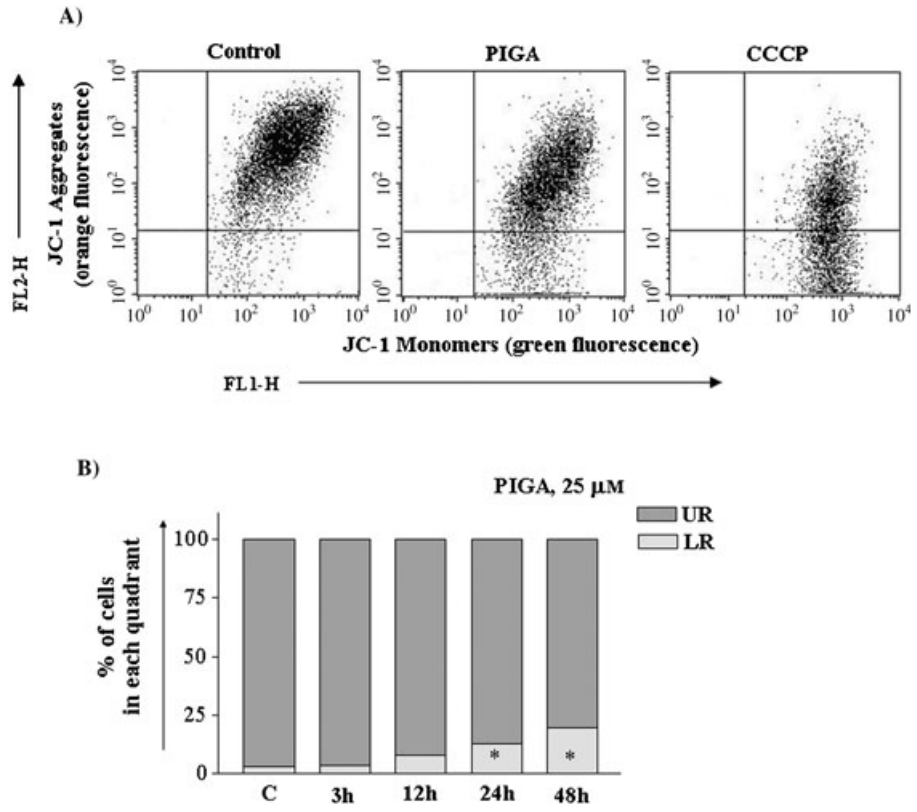

Figure 3. Flow cytometric analysis of mitochondrial transmembrane potential in PIGA-treated C6 glioma cells. A) Representative examples of the fluorescence patterns of treated and untreated C6 glioma cells stained with JC-1. Cells with polarized mitochondria are found in the upper right (UR) quadrant of plots, corresponding to high fluorescence emission in both FL 1 (green; *x*-axis) and FL 2 (orange; *y*-axis) channels. After CCCP (5 μM, 30 min) or PIGA (25 μM, 24 h) treatment, mitochondrial depolarization is evident as a decrease in the fluorescence emission in the FL 2 and an increase in the FL 1 channels, lower right (LR) quadrant. B) C6 glioma cells were treated with PIGA (25 μM) for graded time periods (3–48 h) and $\Delta\Psi$m was evaluated by cytofluorimetric analysis of JC-1-stained cells (as above). Histograms show mean values of cell percentages either in the UR (polarized mitochondria) or in the LR (depolarized mitochondria) quadrant of $\Delta\Psi$m analysis plots derived from three independent experiments. *) $P < 0.05$ with respect to corresponding control, one-way ANOVA (Newman–Keuls test).

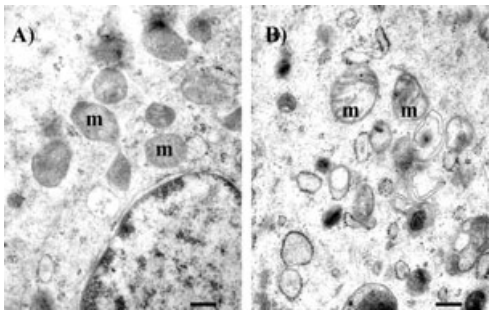

Figure 4. Effect of PIGA on mitochondrial morphology. A) Detail of an untreated C6 glioma cell with several mitochondria in the perinuclear region, exhibiting electron-dense matrices and well organized cristae. B) Detail of a PIGA-treated (25 μM) C6 glioma cell, showing swollen and pale mitochondria. m: mitochondrion. Scale bars: 0.25 μm (A, B).

KCN for 4 h, used as positive control (34.9 ± 3.48 %, $P < 0.01$; Figure 5).[31] Cytochrome c can exit from mitochondria through voltage-dependent anion channels,[32] which is itself associated with mBzR in the mitochondrial outer membrane,[33] and could trigger apoptosis in response to PIGA cell treatment.

Activation of caspase-3

Apoptosis induction was confirmed by caspase-3 activation[34] induced by PIGA cell treatment. The increase in caspase-3 specific activity was 2.81 ± 0.03 ($P < 0.001$), normalized to the control. Moreover, preincubation of PIGA-treated cells with the caspase-3-inhibitor Z-VAD-FMK (50 μM) completely prevented the activation of caspase-3 (0.95 ± 0.21; Figure 6).

Induction of DNA fragmentation

DNA-specific PI staining showed that treatment with PIGA caused a significant increase in the percentage of cells with hypodiploid DNA content, a clear sign of apoptosis, as shown in the frequency histograms from a representative flow cytometric experiment (Figure 7). In particular, the quantity of apoptotic cells (sub-G_0 cells) observed after 25 μM PIGA exposure for 24 h increased to 15.9 ± 2.21 % ($P <$ 0.001) as compared to the control (1.41 ± 0.27 %).

Ultrastructural analysis confirmed that PIGA had induced nuclear fragmentation. Untreated cells were irregularly round with large nuclei, sometimes convoluted or even segmented and mainly euchromatic (Figure 8 A). Cells treated with 25 μM PIGA for 24 h showed a peculiar process, consistent with an intense and progressive blebbing at the nuclear level. In particular, nuclear material surrounded by the internal nuclear membrane was released into the perinuclear space. Thereafter, the vesicles containing chromatin were blebbed in the cytoplasm and appeared surrounded by the external membrane of the nuclear envelope (Figure 8 B). After 72 h of treatment the blebbing process was conspicuous and a number of vesicles surrounded by a double membrane had been released into the cytoplasm (Figure 8 C). Chromatin condensation and margination, typical features of apoptosis, were visible only after prolonged exposure to PIGA (data not shown). Kraici et al.[35] have reported that exposure of glioma cells to the cytostatic dose of cisplatin induces apoptotic cell death with a morphological pattern similar to that observed in PIGA-treated cells (i.e., progressive nuclear degeneration involving both rearrangements of the nuclear envelope and formation of nuclear vesicles).

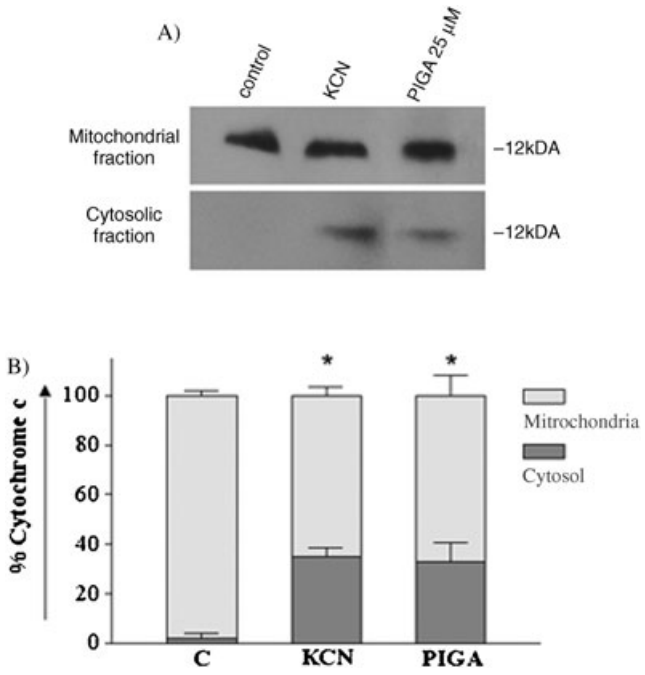

Figure 5. Evaluation of cytochrome c release from mitochondria: C6 glioma cells were exposed to either 25 μM PIGA (24 h) or 3.8 mM KCN (4 h). A) Cytochrome c was detected by Western blot analysis with use of a specific monoclonal antibody as a 12 kDa protein band in both mitochondrial and cytosolic fractions obtained from treated and untreated cells. B) For each individual sample, the immunoreactive band was analysed densitometrically, hence determining the percentages of cytochrome c in the cytosolic and the mitochondrial fractions as a proportion of the total. *) $P < 0.05$ with respect to control, one-way ANOVA (Newman–Keuls test).

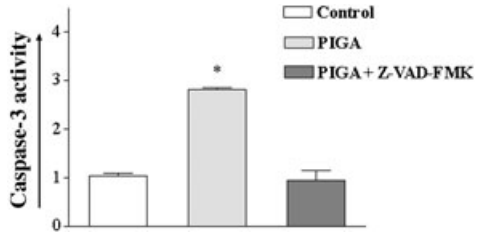

Figure 6. Caspase-3 activity in PIGA-treated C6 glioma cells. After exposure to PIGA (25 μM) in the presence or absence of the caspase inhibitor Z-VAD-FMK (50 μM) for 24 h, caspase-3 specific activity was determined by evaluating cleavage of the specific substrate Ac-DEVD-pNA and release of pNA at 405 nm, as described in the Experimental Section. The data were normalized to the control (arbitrary value = 1) and expressed as means ± SEM derived from at least three separate experiments, performed in duplicate. *) $P < 0.05$ with respect to control, one-way ANOVA (Newman–Keuls test).

Conclusion

Along the 2-phenylindol-3-ylglyoxylamides series, we characterized the derivative *N*,*N*-di-*n*-butyl-5-chloro-2-(4-chlorophenyl)indol-3-ylglyoxylamide (PIGA) as a novel compound with proapoptotic activity against rat C6 glioma cells.

By using different experimental approaches, we determined that PIGA glioma cell treatment induced an apoptotic pattern of cell death. In particular, the dissipation of $\Delta\Psi$m and the cytochrome c release induced by PIGA, together with the almost exclusive mitochondrial localization of the receptor, suggested the ability of PIGA to activate a mitochondrial apoptotic pathway by modulation of MPT-pore opening in this cell line.

The ability of mBzR ligands to induce apoptotic cell death at micromolar concentrations has been well documented in multidrug resistant cells[12,14] and in several cancer cell lines,[7,9,11,16] but this is the first study concerning apoptosis induction in C6 glioma cells with a novel mBzR ligand capable of inducing cell death by itself, independently of other proapoptotic stimuli. Since malignant gliomas, the most common brain tumours characterized by invasive cancer cells that are often refractory to classical therapies, the identification of new ligands with proapoptotic activity may be of relevance.

Our study reports a novel mBzR compound useful for studying MPT pore functioning and with potential therapeutic action against glial tumours.

Experimental Section

Synthesis of PIGA, *N*-*n*-propyl-2-phenylindol-3-ylglyoxylamide and 1-(2-phenyl-1*H*-indol-3-yl)-2-pyrrolidin-1-ylethane-1,2-dione: See the Supporting Information.

Cell culture and mBzR ligand treatments: Rat C6 glioma cells (kindly gifted by Prof. Damir Janigro, Cleveland Clinic Foundation, Cleveland, OH) were cultured in Dulbecco's Modified Eagles Medium (DMEM) as previously described.[11] For treatment, medium was replaced either with complete medium (untreated control cells) or with complete medium supplemented with different PIGA concentrations (ranging from 1 nM to 100 μM) for different times (3–72 h).

mBzR ligands were dissolved in dimethyl sulfoxide (< 1% *v*/*v* of medium). We verified that cell viability remained unaffected under such conditions.

After treatments, both floating and adherent mild-trypsinized cells were collected by centrifugation and used for further analysis.

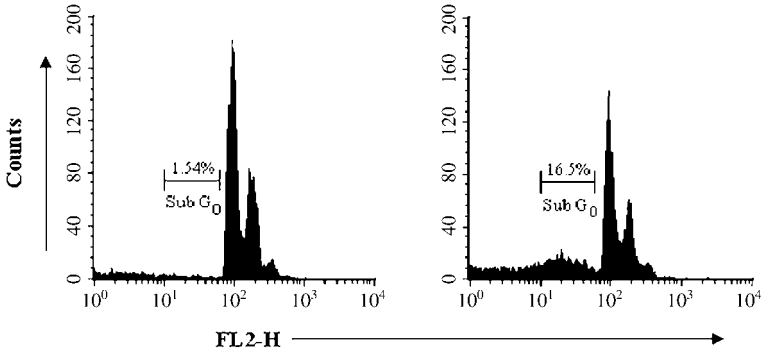

Figure 7. Flow cytometric analysis of DNA content in PIGA-treated C6 glioma cells. Cells were incubated with 25 μM PIGA for 24 h. After incubation, treated and untreated cells were stained with PI, as described in the Experimental Section, and were analysed for DNA content with a FASCcalibur flow cytometer (Becton Dickinson, USA) in the FL 2 channel on a logarithmic scale. DNA content frequency histograms from a representative experiment are shown. Similar data were obtained from four independent experiments.

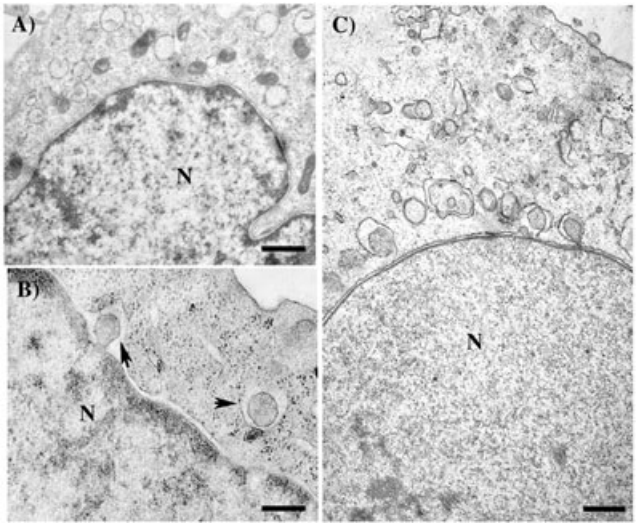

Figure 8. TEM micrographs of nuclear blebbing in PIGA-treated C6 glioma cells. A) Morphological features of untreated control cells showing a mainly euchromatic nucleus and a well preserved cytoplasm containing several mitochondria and vesicles of the endoplasmic reticulum. B) Detail of the perinuclear area of a PIGA-treated C6 glioma cell. Arrows indicate the formation and release of nuclear vesicles into the cytoplasm. C) Conspicuous nuclear blebbing in cells treated with 25 μM PIGA for 72 h. N: nucleus. Scale bars: 1.2 μm (A), 0.4 μm (B), and 1 μm (C).

Cell viability analysis by MTS conversion and trypan blue exclusion assays: Cells were seeded in 96-well plates. After treatment, the number of living cells was estimated by quantitative colorimetric MTS conversion assay (Cell Titer 96® AQueous One Solution Cell Proliferation assay, Promega, Italy), according to manufacturer's instructions. After 2 h of incubation with the MTS reagent, absorbance was measured at 490 nm with a microplate reader (Wallac Victor 2, 1420 Multilabel Counter, Perkin Elmer, USA). All measurements were performed in duplicate, and each experiment was repeated at least three times.

Cell viability was also measured by trypan blue exclusion assay.[36]

Cytofluorimetric analysis of mitochondrial membrane potential: Changes in $\Delta\Psi$m were analysed by use of the fluorescent dye JC-1, as previously described.[11] J-aggregate and J-monomer fluorescence were recorded with a FACScalibur flow cytometer (Becton Dickinson, USA) in fluorescence channel 2 (FL 2) and channel 1 (FL 1), respectively. Necrotic fragments were gated out electronically on the basis of morphological characteristics observed on the forward *vs* side light scatter dot plot.

As a positive control, cells were incubated in the presence of the uncoupling agent CCCP (5 μM) in each experiment.

Evaluation of cytochrome c release from mitochondria: Cell cytosolic and mitochondrial fractions were isolated by use of a mitochondria/cytosol fractionation kit (BioVision; Vinci-Biochem, Italy), according to the manufacturer's instructions, with minor modifications. The protein content of each fraction was determined according to Bradford.[37] Protein aliquots (40 μg) were size-fractionated by SDS-PAGE in acrylamide gel (12%) and electroblotted onto a nitrocellulose membrane. The membrane was blocked overnight in TBS (10 mM Tris-HCl, pH 8, 150 mM NaCl) containing Tween 20 (0.05%) and non-fat dry milk (10%; blocking solution) and was then probed with a monoclonal mouse anti-cytochrome c antibody (1:400; Santa Cruz Biotechnology Inc., USA). After washing with TBS containing Tween 20 (0.05%; TTBS), the membrane was incubated with HSP-conjugated IgG anti-mouse antibody (1:35000; Pierce Biotechnology Inc., USA) and then washed with TTBS. Reactive proteins were visualized with enhanced chemiluminescence SuperSignal West Pico Substrate (Pierce Biotechnology Inc., USA). Quantification of cytochrome c (12 kDa immunoreactive band) was performed by densitometric scanning of autoradiograms with an image analysis system (GS-670 BIO-RAD).

Measurement of caspase-3 activity: Caspase-3 activity was measured with a spectrophotometric assay kit (CaspACE Assay System, Colorimetric Promega, Italy). Briefly, after incubation (24 h) in PIGA (25 μM), with or without caspase inhibitor Z-VAD-FMK (50 μM), cells were collected by centrifugation. Pellets were suspended in cell lysis buffer (supplied with the kit), exposed to repeated freeze/thawing cycles and incubated on ice for 30 min. Insoluble fractions were discarded by centrifugation (5 min at 10000 *g*) and the protein contents in the supernatants were determined.[37] The assay was carried out in 96-well plates, protein extracts (50–60 μg) being incubated in a total volume (100 μL) of assay buffer at 37 °C for 4 h, in the presence of the *para*-nitroaniline conjugated caspase-3 substrate (Ac-DEVD-pNA). The absorbances of individual samples were measured by microplate reader at 405 nm. Caspase-3 specific activity was calculated by use of a pNA standard curve, as pmol of pNA released per hour per mg of proteins. The fold increase of caspase-3 activity was determined by normalizing treated samples to untreated controls.

Samples were run in duplicate, and three independent experiments were performed.

Cytofluorimetric analysis of DNA content: DNA content was evaluated straight after treatment by propidium iodide (PI) DNA staining, followed by flow cytometric analysis. The percentage of apoptotic cells was estimated as previously described.[11] For cell cycle analysis, the cells were seeded at appropriate densities to ensure they had not reached confluency and were therefore out of the log phase of growth prior to their analysis by FACS, performed by use of the ModFit LT software program to evaluate the percentage of cells in each cell cycle phase.

Transmission electron microscopy analysis: After treatment with PIGA (25 μM) at different incubation times, cells were collected by centrifugation. The pellets were washed with phosphate buffered saline (PBS), fixed and embedded in "Epon-Araldite" mixture as previously described.[11] Ultrathin sections were placed on Formvar carbon-coated nickel grids, stained with uranyl acetate and lead citrate, and observed under a Jeol 100 SX transmission electron microscope (Jeol, Ltd, Japan).

Immunocytochemistry and fluorescence microscopy analyses: Cells, grown on glass coverslips, were fixed in paraformaldehyde (4%) at room temperature for 30 min, washed in PBS and blocked in PBS containing Triton X-100 (0.1%) and bovine serum albumin (0.5%; blocking solution). The cells were incubated for 1 h at room temperature in blocking solution containing anti-mBzR antibody (Santa Cruz Biotechnology Inc., USA, 1:50), anti-cytochrome c antibody (Santa Cruz, 1:50) and anti-lamin A antibody (Santa Cruz, 1:50; Santa Cruz Biotechnology Inc., USA). Control cells were incubated in blocking solution with no primary antibody. After washing, the cells were incubated for 1 h at room temperature in blocking solution with FITC-conjugate anti-mouse secondary antibody (1:200; Molecular Probes, NL) and rhodamine-conjugate anti-rabbit secondary antibody (1:200; Santa Cruz Biotechnology Inc., USA). The cells were washed in PBS and mounted for microscope analysis.

To investigate subcellular mBzR distribution in living cells, the cells were grown to confluence on glass coverslips and were then incubated for 45 min in fluorescent ligand NBD-FGIN-1–27 (1 μM; Alexis, Vinci-Biochem, Italy), as previously described.[38]

Data analysis: The nonlinear multipurpose curve-fitting program Graph-Pad Prism was used for data analysis and graphic presentations. All data are presented as mean ± SEM. Statistical analysis was performed by one-way ANOVA (with post hoc Newman Keuls test). $P < 0.05$ was considered statistically significant.

Acknowledgement

This work was supported by a Grant from the Italian MURST (Cofinanziamento Programmi di Ricerca di Interesse Nazionale) to C.M. and V.G.

Keywords: amides · apoptosis · DNA damage · mitochondria · permeability transition · receptors

[1] B. Amirlak, W. T. Couldwell, *J. Neuro-Oncol.* **2003**, *63*, 129 – 145.
[2] D. R. Green, J. C. Reed, *Science* **1998**, *281*, 1309 – 1312.
[3] P. Casellas, S. Galiegue, A. S. Basile, *Neurochem. Int.* **2002**, *40*, 475 – 486.
[4] P. J. Marangos, J. Patel, J. P. Boulenger, R. Clark-Rosenberg, *Mol. Pharmacol.* **1982**, *22*, 26 – 32.
[5] G. Le Fur, N. Vaucher, M. L. Perrier, A. Flamier, J. Benavides, C. Renault, M. C. Dubroeucq, A. Uzan, *Life Sci.* **1983**, *33*, 449 – 457.
[6] D. A. Fennell, M. Corbo, A. Pallaska, F. E. Cotter, *Br. J. Cancer* **2001**, *84*, 1397 – 1404.
[7] K. Maaser, M. Hopfner, A. Jansen, G. Weisinger, M. Gavish, A. P. Kozikowski, A. Weizman, P. Carayon, E. O. Riecken, M. Zeitz, H. Scherubl, *Br. J. Cancer* **2001**, *85*, 1771 – 1780.
[8] A. P. Sutter, K. Maaser, M. Hopfner, B. Barthel, P. Grabowski, S. Faiss, P. Carayon, M. Zeitz, H. Scherubl, *Int. J. Cancer* **2002**, *102*, 318 – 327.
[9] A. P. Sutter, K. Maaser, B. Barthel, H. Scherubl, *Br. J. Cancer* **2003**, *89*, 564 – 572.
[10] A. P. Sutter, K. Maaser, B. Gerst, A. Krahn, M. Zeitz, H. Scherubl, *Biochem. Pharmacol.* **2004**, *67*, 1701 – 1710.
[11] B. Chelli, A. Lena, R. Vanacore, E. Da Pozzo, B. Costa, L. Rossi, A. Salvetti, F. Scatena, S. Ceruti, M. P. Abbracchio, V. Gremigni, C. Martini, *Biochem. Pharmacol.* **2004**, *68*, 125 – 134.
[12] T. Hirsch, D. Decaudin, S. A. Susin, P. Marchetti, N. Larochette, M. Resche-Rigon, G. Kroemer, *Exp. Cell Res.* **1998**, *241*, 426 – 434.
[13] D. E. Banker, J. J. Cooper, D. A. Fennell, C. L. Willman, F. R. Appelbaum, F. E. Cotter, *Leuk. Res.* **2002**, *26*, 91 – 106.
[14] D. E. Muscarella, K. A. O'Brien, A. T. Lemley, S. E. Bloom, *Toxicol. Sci.* **2003**, *74*, 66 – 73.
[15] S. Galiegue, N. Tinel, P. Casellas, *Curr. Med. Chem.* **2003**, *10*, 1563 – 1572.
[16] W. Xia, S. Spector, L. Hardy, S. Zhao, A. Saluk, L. Alemane, N. L. Spector, *Proc. Natl. Acad. Sci. USA* **2000**, *97*, 7494 – 7499.
[17] G. Primofiore, F. Da Settimo, S. Taliani, F. Simorini, M. P. Patrizi, E. Novellino, G. Greco, E. Abignente, B. Costa, B. Chelli, C. Martini, *J. Med. Chem.* **2004**, *47*, 1852 – 1855.
[18] A. P. Kozikowski, D. Ma, J. Brewer, S. Sun, E. Costa, E. Romeo, A. Guidotti, *J. Med. Chem.* **1993**, *36*, 2908 – 2920.
[19] W. J. Houlihan, V. A. Parrino, Y. Uike, *J. Org. Chem.* **1981**, *46*, 4511 – 4515.
[20] M. Landau, A. Weizman, E. Zoref-Shani, E. Beery, L. Wasseman, O. Landau, M. Gavish, S. Brenner, J. Nordenberg, *Biochem. Pharmacol.* **1998**, *56*, 1029 – 1034.
[21] I. Carmel, F. A. Fares, S. Leschiner, H. Scherubl, G. Weisinger, M. Gavish, *Biochem. Pharmacol.* **1999**, *58*, 273 – 278.
[22] M. Gavish, I. Bachman, R. Shoukrun, Y. Katz, L. Veenman, G. Weisinger, A. Weizman, *Pharmacol. Rev.* **1999**, *51*, 619 – 640.
[23] D. M. Zisterer, G. Campiani, V. Nacci, D. C. Williams, *J. Pharmacol. Exp. Ther.* **2000**, *293*, 48 – 59.
[24] E. Hosli, W. Ruhl, L. Hosli, *Int. J. Dev. Neurosci.* **2000**, *18*, 101 – 111.
[25] A. M. Gorman, G. B. O'Beirne, C. M. Regan, D. C. Williams, *J. Neurochem.* **1989**, *53*, 849 – 855.
[26] D. M. Zisterer, N. Hance, G. Campiani, A. Garofalo, V. Nacci, D. C. Williams, *Biochem. Pharmacol.* **1998**, *55*, 397 – 403.
[27] D. Kletsas, W. Li, Z. Han, V. Papadopoulos, *Biochem. Pharmacol.* **2004**, *67*, 1927 – 1932.
[28] K. Maaser, A. P. Sutter, A. Krahn, M. Hopfner, P. Grabowski, H. Scherubl, *Biochem. Biophys. Res. Commun.* **2004**, *324*, 878 – 886.
[29] M. Hardwick, D. Fertikh, M. Culty, H. Li, B. Vidic, V. Papadopoulos, *Cancer Res.* **1999**, *59*, 831 – 842.
[30] R. C. Brown, B. Degenhardt, M. Kotoula, V. Papadopoulous, *Cancer Lett.* **2000**, *156*, 125 – 132.
[31] S. Ceruti, D. Barbieri, E. Veronese, F. Cattabeni, A. Cossarizza, A. M. Giammarioli, W. Malorni, C. Franceschi, M. P. Abbracchio, *J. Neurosci. Res.* **1997**, *47*, 372 – 383.
[32] S. Shimizu, M. Narita, Y. Tsujimoto, *Nature* **1999**, *399*, 483 – 487.
[33] M. W. McEnery, A. M. Snowman, R. R. Trifiletti, S. H. Snyder, *Proc. Natl. Acad. Sci. USA* **1992**, *89*, 3170 – 3174.
[34] G. Kroemer, B. Dallaporta, M. Resche-Rigon, *Annu. Rev. Physiol.* **1998**, *60*, 619 – 642.
[35] D. Krajci, V. Mares, V. Lisa, A. Spanova, J. Vorlicek, *Eur. J. Cell Biol.* **2000**, *79*, 365 – 376.
[36] S. Ruan, M. F. Okcu, R. C. Pong, M. Andreeff, V. Levin, J. T. Hsieh, W. Zhang, *Clin. Cancer Res.* **1999**, *5*, 197 – 202.
[37] M. M. Bradford, *Anal. Biochem.* **1976**, *72*, 248 – 254.
[38] A. P. Kozikowski, M. Kotoula, D. Ma, N. Boujrad, W. Tuckmantel, V. Papadopoulos, *J. Med. Chem.* **1997**, *40*, 2435 – 2439.

Received: October 1, 2004

